

# Monte Carlo Studies of Self-Interacting Polymer Chains with Excluded Volume. I. Squared Radii of Gyration and Mean-Square End-to-End Distances and Their Moments

Frank L. McCrackin,\* Jacob Mazur, and Charles M. Guttman

*Institute for Materials Research, National Bureau of Standards, Washington, D. C. 20234.  
Received August 13, 1973.*

**ABSTRACT:** Random walks that are not allowed to intersect themselves were generated on the simple cubic and face-centered cubic lattices and used as a model of a linear polymer chain in dilute solution with excluded volume and attractive energies between the chain elements. The mean-square end-to-end distances and mean-squared radii of gyration and their moments were computed for chain lengths up to 2000 segments and for a wide range of attractive energies. The partition functions of the chains were also computed. The attractive energy required for a given property of the chain to be the same as the given property of a random coil, the  $\Theta$  point, was investigated. The required attractive energy depended slightly on the particular property chosen for comparison, so rather than a unique  $\Theta$  point, a narrow range of  $\Theta$  points was found.

The only analytically soluble model of a polymer in solution which takes the connectivity of the polymer into account is the random walk model. This view of a polymer in solution disregards both attractive and repulsive interaction between unbonded polymer segments and between the polymer and the solvent. In fact, in this model many polymer segments are allowed to occupy the same spatial point. Because analytical theories of polymer configurations cannot account for even the fact that only one polymer segment may occupy a given point (the so-called excluded volume effect) in an exact manner, numerous studies of polymer configurations simulated by Monte Carlo calculations on non-self-intersecting random walks<sup>1-6</sup> have been performed. Most of these calculations have considered the volume exclusion problem alone and have not included in the calculations attractive energies between segments. Furthermore, most of these calculations have investigated  $\langle R^2 \rangle$ , the mean-square end-to-end distance, although the squared radius of gyration  $\langle S^2 \rangle$ , is more closely related to such interesting polymer properties as diffusion, viscosity, and light scattering.<sup>7</sup>

In this paper we shall present Monte Carlo calculations of configurations using a modification of the technique of Rosenbluth and Rosenbluth<sup>6</sup> to generate non-self-intersecting chains on a lattice. The values of  $\langle R^2 \rangle$  and  $\langle S^2 \rangle$  were computed for a wide range of attractive energies,  $\epsilon$ , between the nonbonded segments of the chains separated by the lattice spacing and for chain lengths up to 2000 segments. (To our knowledge this is the first time  $\langle S^2 \rangle$  has been computed as a function of  $\epsilon$ .) The distribution of  $\langle R^2 \rangle$  and  $\langle S^2 \rangle$  was investigated by calculations of higher moments of distributions in  $R$  and  $S$ . Finally, the partition function per segment of the chains was obtained. These calculations were performed for chains on the simple cubic and face-centered cubic lattices.

For non-self-reversing chains without excluded volume (a random-coil model of a polymer), it has been shown<sup>8</sup>

previously that for chains of a large number  $N$  of segments on a simple cubic lattice

$$\langle R^2 \rangle = 3N/2 \quad (1)$$

$$\langle S^2 \rangle = N/4 \quad (2)$$

and on the face-centered cubic lattice

$$\langle R^2 \rangle = 6N/5 \quad (3)$$

$$\langle S^2 \rangle = N/5 \quad (4)$$

For chains with excluded volume and with zero or small attractive energy between unbonded segments, previous workers<sup>1-6</sup> have found that their  $\langle R^2 \rangle$  data for large chain lengths obeyed

$$\langle R^2 \rangle = AN^{\gamma_R} \quad (5)$$

In eq 5,  $A$  and  $\gamma_R$  depend on  $\Phi = -\epsilon/k_B T$ , where  $\epsilon$  is the attractive energy between unbonded segments separated by one lattice distance,  $k_B$  is Boltzmann constant, and  $T$  is the temperature. The attractive energy for segments more than one lattice distance apart is assumed to be zero. In this paper we have verified eq 5. Moreover, we found that

$$\langle S^2 \rangle = BN^{\gamma_S} \quad (6)$$

where  $B$  and  $\gamma_S$  also depend on  $\Phi$ . Furthermore, we find that for any given  $\Phi$

$$\gamma_R = \gamma_S = \gamma \quad (7)$$

For chains with excluded volume but no attractive energies ( $\Phi = 0$ ),  $\gamma$  is found to be 1.2 in this and previous investigations<sup>1-6</sup> for all the lattices investigated. For increasing attractive energy between segments,  $\gamma$  decreases smoothly until for a certain value of  $\Phi$ ,  $\Phi = \Phi_c$ ,  $\gamma$  becomes 1, the value for chains without excluded volume. In deference to common usage in the literature,<sup>8</sup> we will call this condition the " $\Theta$  point." The simplistic view of the  $\Theta$  point is that point of temperature and attractive energy between segments,  $\Phi = \Phi_c$ , at which the attractive energy compensates for the excluded volume in a way such that the configurational properties of long chains are the same as for those without excluded volume. From this view, the values of  $\gamma$ ,  $A$ , and  $B$ , the distribution of  $R^2$  and  $S^2$ , and the partition function of the chains should have the same values at the  $\Theta$  point as the free-coil model. This view will be tested in this paper.

Although this and most similar Monte Carlo investigations consider chains on a lattice for ease of computation,

- (1) F. T. Wall, S. Windwer, and P. J. Gans, "Methods in Computational Physics," Vol. 1, Academic Press, Inc., New York, N. Y., 1963.
- (2) A. I. Medalia in "Surface and Colloid Science," Vol. 3, E. Matijevic, Ed., John Wiley and Sons, New York, N. Y., 1971.
- (3) Z. Alexandrowicz, *J. Chem. Phys.*, **51**, 561 (1969).
- (4) H. E. Warvari, K. K. Knaell, and R. A. Scott, III, *J. Chem. Phys.*, **56**, 2903 (1972).
- (5) J. Mazur and F. L. McCrackin, *J. Chem. Phys.*, **49**, 648 (1968).
- (6) M. N. Rosenbluth and A. W. Rosenbluth, *J. Chem. Phys.*, **23**, 356 (1955).
- (7) C. Tanford, "Physical Chemistry of Macromolecules," John Wiley & Sons, Inc., New York, N. Y., 1961.
- (8) P. J. Flory, "Statistical Mechanics of Chain Molecules," Interscience Publishers, New York, N. Y., 1969.

one desires to obtain information concerning real polymer molecules that are not restricted to a lattice model. Therefore, in this paper we look for parameters or trends that are obtained for both choices of lattices we have used in the expectation that such trends will also apply to real polymer molecules. An example of such a lattice-independent parameter is the aforementioned  $\gamma$  for chains with excluded volume but without attractive energies, which has been found to have the same value (1.2) for all lattices investigated so far.

The next section gives the details of computations. The remaining sections give the results and their discussion.

**Description of Computations.** Polymer molecules were simulated on a computer by non-self-intersecting walks on a simple cubic and a face-centered cubic lattice following the method of Rosenbluth and Rosenbluth (R&R).<sup>6</sup> The method of R&R has been found to be especially efficient near the  $\Theta$  point ( $\Phi = \Phi_c$ ).

The general scheme for the program we used has been previously described in detail;<sup>5</sup> to provide the language and foundations to describe some latter modifications in our approach, we shall sketch here the fundamental program. The first step of the walk is placed near the center of the lattice; before each further step of the walk, each possible direction for the step is examined for intersection with previous steps. A list of all directions which do not cause intersections is made (called allowed vectors). A random choice of the allowed vectors is made and a step is taken in the chosen direction. After a walk of the desired length is generated, parameters of the walk of physical interest, such as number of nearest-neighbor contacts, end-to-end distance, and radius of gyration, are recorded. We devised an efficient method, given in Appendix A, for calculating the radius of gyration.

Because the above scheme does not generate all non-self-intersecting walks with equal probabilities, we must separately weight each walk when calculating averages of the parameters over many walks.<sup>6</sup> Since we shall further modify the above described method of generating non-self-intersecting walks, we shall then need to modify the weights; therefore we now review the method of computing weights for the R&R method.

Let  $\sigma$  be the maximum number of choices for a step of the walk without immediate reversals; thus  $\sigma = 5$  for the simple cubic lattice and  $\sigma = 11$  for the face-centered lattice. When two positions of the walk not connected by a single step lie a distance equal to the lattice spacing from each other, they are said to form a contact. Let the  $(i - 1)$ th step of a walk form  $C_i$  contacts. Then the  $i$ th step can be in  $\sigma - C_i$  different directions without the walk intersecting itself. In the R&R method of generating the walks, a random choice for the  $i$ th step is made of these possible directions; each choice has the *a priori* probability  $1/(\sigma - C_i)$ . The first step may be taken in  $\sigma + 1$  directions. Thus the probability of generating a particular walk is

$$\frac{1}{\sigma + 1} \prod_{i=2}^N \frac{1}{\sigma - C_i}$$

the weight of the walk is the reciprocal of the probability and so is given by

$$(\sigma + 1) \prod_{i=2}^N (\sigma - C_i)$$

For a sample of  $m$  walks, the weight of the  $k$ th walk is then

$$w_k = (\sigma + 1) \prod_{i=2}^N (\sigma - C_{ik}) \quad (8)$$

where  $C_{ik}$  is the number of contacts formed by the  $(i - 1)$ th step of the  $k$ th walk. The estimate of the partition function of a single chain is

$$f = \frac{1}{m} \sum_{k=1}^m w_k \exp(P_k \Phi) \quad (9)$$

where

$$P_k = \sum_{i=2}^N C_{ik} \quad (10)$$

is the total number of contacts in the  $k$ th walk. The estimate of the average value of any calculated property  $v$  of the walks is<sup>6</sup>

$$\langle v \rangle = \frac{\sum_{k=1}^m v_k w_k \exp(P_k \Phi)}{\sum_{k=1}^m w_k \exp(P_k \Phi)} \quad (11)$$

where  $v_k$  is the value of the parameter for the  $k$ th walk. The weights will have extremely large values for long walks of hundreds of steps. Because the average value of a parameter given by eq 11 is seen to be unchanged if all weights are changed by a constant factor, for computational convenience we redefine  $w_k$  as

$$w_k = \prod_{i=2}^N (\sigma - C_{ik}) / \sigma \quad (12)$$

The estimate given by eq 11 has been shown<sup>9</sup> to be biased for finite sample size, i.e., replicate calculations of  $\langle v \rangle$  for a given sample size  $m$  will scatter around a mean value different than the true value of  $\langle v \rangle$ . However, the estimate has been shown to be asymptotically unbiased, i.e., the bias goes to zero as the sample size  $m$  goes to infinity. A method of estimating the bias from the covariance of the estimate and the partition function is developed in Appendix B. By this method, the bias for all quantities calculated in this paper has been shown to be smaller than their standard deviation; therefore, this bias is neglected.

In order to evaluate the precision of the estimates, the walks were generated in groups, and the partition function and estimates of each group were calculated by eq 9-12. To compute the best value of  $\langle v \rangle$ , the value  $\langle v \rangle_i$  of the  $i$ th group must be weighted by the partition function of that group  $f_i$ , thus

$$\langle v \rangle = \frac{\sum_{i=1}^L f_i \langle v \rangle_i}{\sum_{i=1}^L f_i} \quad (13)$$

where  $L$  is the number of groups.

If all values of  $f_i$  were equal,  $\langle v \rangle$  would be a simple average of  $\langle v \rangle_i$  and the standard deviation,  $s$ , of  $\langle v \rangle_i$  of a group would be

$$s^2 = \sum_{i=1}^L (\langle v \rangle_i - \langle v \rangle)^2 / (L - 1) \quad (14)$$

and the standard deviation of the average of  $v$  over the groups would be given by

$$s^2_{\langle v \rangle} = \sum_{i=1}^L (\langle v \rangle_i - \langle v \rangle)^2 / L(L - 1) \quad (15)$$

For our data, a sufficiently large number of walks were generated for each group that the values of  $f_i$  were approximately the same for all groups. Therefore eq 15 gives a good approximation of the standard deviation of  $\langle v \rangle$ .

In the usual formula for the standard deviation of a weighted average, the weights are a measure of the accuracy of the individual values, so the squared differences,  $(\langle v \rangle_i - \langle v \rangle)^2$ , are weighted. However, our weights,  $f_i$ , are not a measure of the accuracy of the individual values, but are required to compensate for the fact that all chains are not computed with equal probability. Therefore, the usual formula will not apply to our case and eq 15 must be used.

A more convenient measure of precision is the coefficient of variation given by

$$\text{coef var of } \langle v \rangle = 100s_{\langle v \rangle} / \langle v \rangle \quad (16)$$

which expresses the standard deviation as a percentage of  $\langle v \rangle$ . The coefficient of variation was computed for all calculated parameters of the walks, and only those values for which the coefficient of variation is less than 5% are reported in this paper. However, the coefficient of variation is much less than 5% for most of the reported data.

We have also used the coefficient of variation as a measure of the efficiency of the Monte Carlo calculation at a particular energy. We have found for a given method of generating the chains that the coefficient of variation is strongly dependent on  $\Phi$ , i.e., on temperature and the attractive energy between segments.

The dependence of the precision of  $\langle S^2 \rangle$  on the attractive energy,  $\Phi$ , is illustrated in Figure 1. Here the mean-square radii of gyration of 500 walks on the simple cubic lattice of 100 steps each and for values of  $\Phi$  from 0 to 1 were computed using the method of R&R. The calculation was repeated 19 times so that 20 values, each based on 500 walks, of the mean-square radius of gyration were obtained for each value of  $\Phi$ . The coefficients of variation calculated from these mean values by eq 15 and 16 are shown in Figure 1 vs.  $\Phi$ . They are seen to have a minimum near the  $\Theta$  point,  $\Phi_c$ , and to be very large for large values of  $\Phi$ . This suggests that the R&R method works best near  $\Phi = \Phi_c$ . In fact we have found that in the vicinity of  $\Phi_c$ , using the R&R method we have been able to extend our data to very long chain lengths with high precision. (In Appendix C we suggest why this might be true.)

The substantial increase in the coefficient of variation for high energies is thought to be due to the terms  $\exp(P_k\Phi)$  in eq 11. This term is large for large  $P_k$ , i.e., for tightly coiled walks with many contacts. If  $\Phi$  is large, the few terms in the summand which correspond to large  $P_k$  are orders of magnitude larger than the rest of the terms, so only the walks corresponding to these terms contribute to the calculation of the mean value of the parameter. Thus, although 10,000 walks were originally generated and used for the calculation, the estimated values actually depended on only relatively few walks and are therefore very imprecise for high  $\Phi$ . The variation of the precision with  $\Phi$  is further discussed in Appendix C.

In order to determine the values of parameters for walks with large attractive energies (large values of  $\Phi$ ), the original method of generating the walks was changed so that more important walks, i.e., walks containing many contacts, were generated. The methods developed for this purpose are examples of Importance Sampling. The proper weights,  $w_k$ , will no longer be given by eq 12 but will depend on the rules used for generating the chains and are easily computed.<sup>9</sup>

Importance sampling was first applied to random walks on a lattice by Wall, Windwer, and Gans.<sup>1</sup> They chose the left, right, and trans steps on a tetrahedral lattice with different probabilities so that when dealing with attractive energies the generated walks would be more coiled and would contain more contacts than walks generated

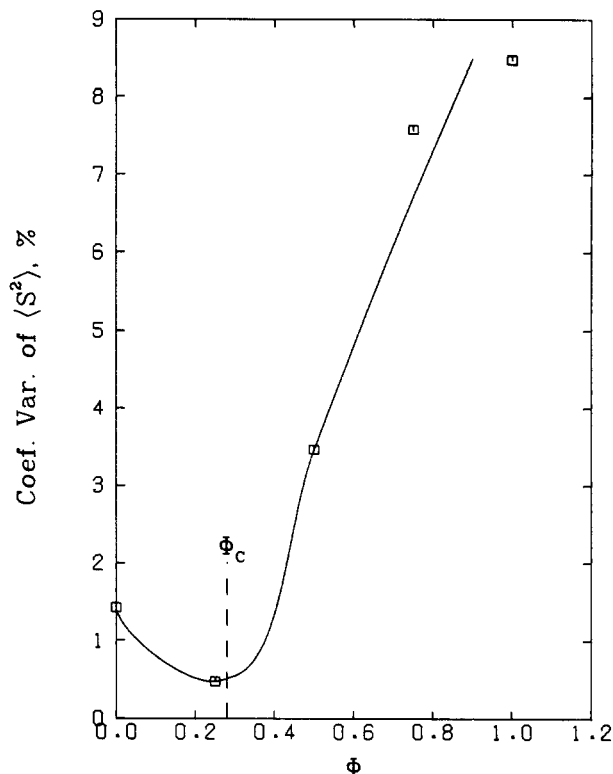


Figure 1. Coefficient of variation of the mean-squared radius of gyration,  $\langle S^2 \rangle$ , vs.  $\Phi$  for chains of 100 segments on the simple cubic lattice using method of R&R. Notice the minimum near  $\Phi = 0.25$ . The solid curve is schematic.

without importance sampling. However, they did not report whether more precise estimates of the parameters of the walks for large  $\Phi$  were obtained by this procedure.

We investigated two methods of importance sampling of random walks. In method A, steps taken toward the coordinate of the first site of the walk were chosen with a probability different from the probability for steps taken away from the first site. For example, consider a walk on a cubic lattice started at the lattice site (0,0,0) which after a number of steps reaches the lattice site (3,-5,-4). Furthermore, let the next steps of the walk that are allowed by volume exclusion be  $\Delta x = 1$ ,  $\Delta x = -1$ ,  $\Delta y = 1$ ,  $\Delta z = 1$ , and  $\Delta z = -1$ . Without importance sampling, each of these steps would have the probability of  $1/5$  of being chosen. However, if steps taken toward the coordinate (0,0,0) are given twice the probability of those taken away from (0,0,0), the above steps will have probabilities of  $1/8$ ,  $1/4$ ,  $1/4$ ,  $1/4$ , and  $1/8$ , respectively.

Method A as described above was found to give precise estimates of both  $\langle S^2 \rangle$  and  $\langle R^2 \rangle$  when  $\Phi$  is around 1.0 for the simple cubic lattice, because for this value of  $\Phi$  only tightly coiled configurations are important; however for  $\Phi$  from 0.3 to 0.7 imprecise estimates are obtained, because in this range of  $\Phi$  the important configurations are only slightly coiled configurations. Thus we looked for a method of sampling which gives accurate results in the region  $\Phi = 0.3-0.7$ .

In method B of importance sampling, the probability of an allowable step of a walk being chosen depends on the number of contacts that would be produced by the step rather than on the direction of the step. Before a step is taken, all allowable steps are tested to determine the number of contacts that they would produce. A step that would produce one contact was taken with twice the probability of a step that would produce no contacts; a step that would produce two contacts was taken with three

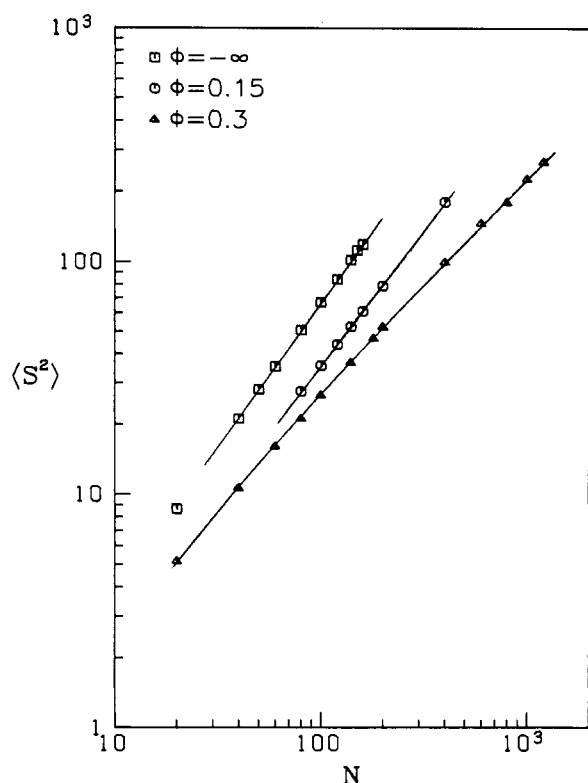


Figure 2.  $\langle S^2 \rangle$  vs. chain length  $N$  for chains on the simple cubic lattice for  $\Phi = -\infty$  (double-excluded volume),  $\Phi = 0.15$  and  $\Phi = 0.30$ .

times the probability of a step that would produce no contacts, etc. Since this procedure produced walks with too many contacts, it was modified to 4-3 weighting. A step that would produce one contact was taken with  $\frac{4}{3}$  the probability of a step that would produce no contact; a step that would produce two contacts was taken with  $\frac{5}{3}$  the probability of a step that would produce no contact; etc.

Obviously method B can be generalized to use different probabilities for each of the possible steps. The form discussed above was found to be particularly effective for  $\Phi = 0.4$  and  $0.5$  in the simple cubic lattice. Method B requires that all allowable steps be tested for contacts before each step is taken, therefore, more calculations are required for it than for method A.

## Results

**Mean-Square Values of  $R^2$  and  $S^2$ .** Figures 2 and 3 show the mean squared radius of gyration  $\langle S^2 \rangle$  and Figures 4 and 5 show the mean squared end-to-end distances,  $\langle R^2 \rangle$ , vs. the number of segments in the chains on a simple cubic lattice on double logarithmic scales. Values of the interaction parameter in these figures range from  $\Phi = -\infty$  (infinite repulsive energy) to  $\Phi = \infty$  (infinite attractive energy). Figures 6 and 7 show similar data on the face-centered cubic lattice. Only data with a coefficient of variation of less than 5% are presented in these figures and are used in the following discussions and fitting procedures.

For the case of infinite repulsive energy between segments ( $\Phi = -\infty$ ), only chains without nearest-neighbor contacts are allowed, *i.e.*, chains with no segments occupying either a previously occupied lattice site or a site within a lattice distance of a previously occupied site. Such double-excluded volume chains were generated on the simple cubic lattice; their values of  $\langle S^2 \rangle$  and  $\langle R^2 \rangle$  are shown in Figures 2 and 4.

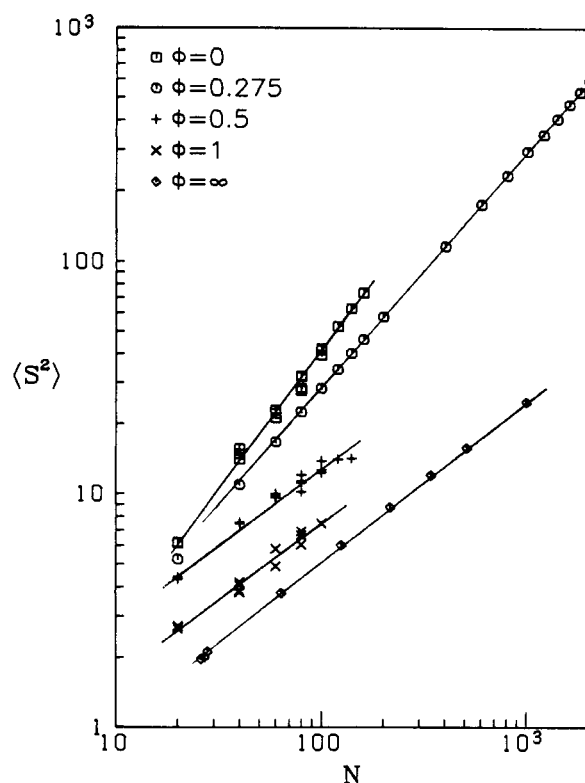


Figure 3.  $\langle S^2 \rangle$  vs.  $N$  for chains on the simple cubic lattice for  $\Phi = 0$ ,  $\Phi = 0.275$ ,  $\Phi = 0.4$ ,  $\Phi = 0.5$ ,  $\Phi = 1$ , and  $\Phi = \infty$ . Notice the long linear region for the three lowest energies.

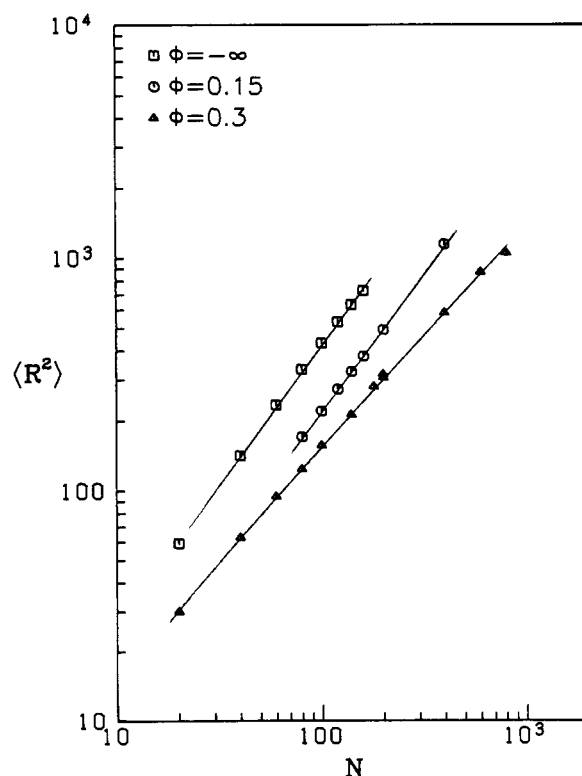


Figure 4. Mean-square end-to-end distances  $\langle R^2 \rangle$  vs.  $N$  for chains on the simple cubic lattice for  $\Phi = \infty$ ,  $0.15$ , and  $0.3$ .

In the case of  $\Phi = +\infty$ , only the configurations with the maximum possible number of contacts are allowed, *i.e.*, the most dense configurations. These configurations are found in Appendix D to have the external shape of a cube

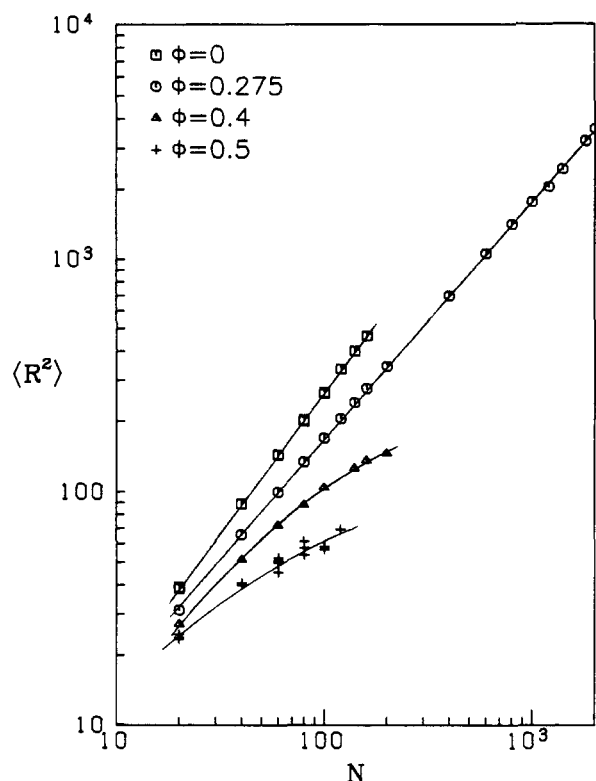


Figure 5. Mean-square end-to-end distances  $\langle R^2 \rangle$  vs.  $N$  for chains on the simple cubic lattice for  $\phi = 0$ ,  $\phi = 0.273$ ,  $\phi = 0.4$ , and  $\phi = 0.5$ .

for the simple cubic lattice. Its radius of gyration, computed in Appendix D, is given in Figure 3 and Table I.

A number of curves on the Figures 2-7 are straight lines for sufficiently long chains, *i.e.*, chains with large  $N$ . Straight lines were also found for curves at other values of  $\phi$  not shown in the figures. We fit these lines using linear squares for the parameters  $A$ ,  $B$ ,  $\gamma_R$ , and  $\gamma_S$  in the following equations, obtained from eq 5 and 6

$$\log \langle R^2 \rangle = \log A + \gamma_R \log N \quad (17)$$

$$\log \langle S^2 \rangle = \log B + \gamma_S \log N \quad (18)$$

The results of this fit for chains on the simple cubic lattice are given in Table I, and for chains on the face-centered cubic lattice are given in Table II. Values of  $N$  from the lowest values for which eq 17 and 18 apply to the largest values for which the coefficients of variations of  $\langle R^2 \rangle$  and  $\langle S^2 \rangle$  are less than 5% were used in the fittings. The range of values of  $N$  used for each fitting is shown in the tables.

To determine the lower limit of  $N$  for which eq 17 and 18 hold, these equations and the deviations of the given values of  $\log \langle R^2 \rangle$  and  $\log \langle S^2 \rangle$  from the calculated values were examined. If the deviations seemed random with respect to  $N$ , the lowest value of  $N$  used was taken to be the lower limit of  $N$ . However, if the deviations showed systematic behavior, for example, if many consecutive deviations were all of the same sign, the range of values of  $N$  was assumed to exceed the range over which eq 17 and 18 apply and the lower limit of  $N$  was increased. This process was repeated until the deviations between given and calculated values of  $\langle R^2 \rangle$  and  $\langle S^2 \rangle$  appeared to be random.

The values of  $\gamma_R$  and  $\gamma_S$  computed from the straight lines of Figures 2-7 are presented in Tables I and II. The values of  $\gamma_R$  and  $\gamma_S$  are seen to be very close for all values of  $\phi$  except for  $\phi = -\infty$ . Even for this case,  $\gamma_R$  and  $\gamma_S$  do not differ significantly because the data for  $\phi = -\infty$  are

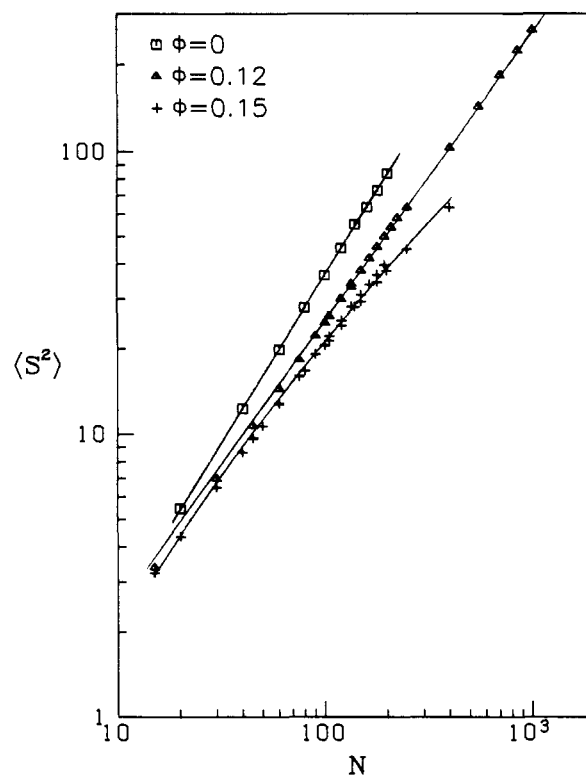


Figure 6.  $\langle S^2 \rangle$  vs.  $N$  for chains on the face-centered lattice for  $\phi = 0$ ,  $\phi = 0.12$ ,  $\phi = 0.15$ , and  $\phi = 0.2$ .

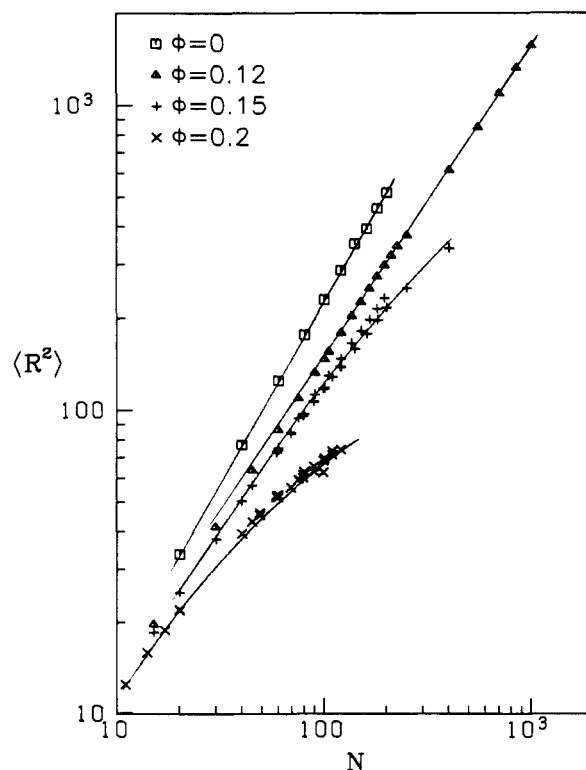


Figure 7.  $\langle R^2 \rangle$  vs.  $N$  for the chains on the face-centered lattice for  $\phi = 0$ ,  $\phi = 0.12$ ,  $\phi = 0.15$ , and  $\phi = 0.2$ .

less accurate than for the other values of  $\phi$ . To test the assumption that  $\gamma_R = \gamma_S$  for a given value of  $\phi$ , we first fitted the curves without assuming that  $\gamma_R$  equals  $\gamma_S$ , and then fitted the same curves assuming  $\gamma_R$  equals  $\gamma_S$ . The fitted parameters  $A$  and  $B$  showed no significant differences in either of these two ways of fitting and equally

Table I  
Fitting of  $\langle R^2 \rangle$  and  $\langle S^2 \rangle$  for the Simple Cubic Lattice to the Equations  
 $\log \langle R^2 \rangle = \log A + \gamma_R \log N$  and  $\log \langle S^2 \rangle = \log B + \gamma_S \log N$

$\Phi$	Range of $N$	$\gamma_R$	$\gamma_S$	$\gamma$	$A$	$B$	Coef of Var (%)
$-\infty$	40-160	1.18	1.25	1.22	1.52	0.237	2.0
0	11-150	1.197	1.196	1.196	1.078	0.170	0.6
0.1	19-500	1.171	1.170	1.170	1.08	0.173	0.7
0.15	20-400	1.161	1.150	1.155	1.08	0.175	1.3
0.24	20-300	1.085	1.082	1.084	1.266	0.2086	0.3
0.25	20-2000	1.074	1.070	1.072	1.296	0.2146	0.6
0.26	120-300	1.047	1.050	1.049	1.42	0.236	0.2
0.275	120-2000	1.0004	1.0006	1.0005	1.69	0.282	0.9
0.29	140-300	$\leq 0.981$	$\leq 0.980$	$\leq 0.980$	1.81	0.306	0.1
$\infty$			0.667			0.25	

Table II  
Fitting of  $\langle R^2 \rangle$  and  $\langle S^2 \rangle$  for the Face-Centered Cubic Lattice to the Equations  
 $\log \langle R^2 \rangle = \log A + \gamma_R \ln N$  and  $\log \langle S^2 \rangle = \log B + \gamma_S \log N$

$\Phi$	Range of $N$	$\gamma_R$	$\gamma_S$	$\gamma$	$A$	$B$	Coef of Var (%)
0	19-200	1.192	1.186	1.190	0.951	0.152	1.19
0.05	20-550	1.153	1.154	1.154	0.980	0.159	1.6
0.1	50-1000	1.098	1.102	1.100	1.033	0.170	1.1
0.11	45-225	1.073	1.075	1.074	1.101	0.183	0.1
0.12	100-1000	1.023	1.027	1.025	1.323	0.222	0.7
0.1225	100-1000	1.015	1.016	1.016	1.340	0.227	1.01
0.125	100-1000	$\leq 0.996$	$\leq 0.994$	$\leq 0.995$	1.464	0.249	0.6
0.1275	100-1000	$\leq 0.977$	$\leq 0.978$	$\leq 0.978$	1.555	0.265	0.98
0.130	135-1000	$\leq 0.938$	$\leq 0.944$	$\leq 0.941$	1.875	0.319	0.94

good fits were obtained in both cases. Thus we feel that wherever the power law described in eq 5 and 6 (or eq 17 and 18) hold,  $\langle S^2 \rangle$  is proportional to  $\langle R^2 \rangle$ .

For larger values of  $\Phi$ ,  $\langle R^2 \rangle$  and  $\langle S^2 \rangle$ , could not be fitted by eq 17 and 18, i.e., the curves in Figures 3 and 6 did not have a linear range in the range of computed values. This seemed to occur for  $\Phi$  larger than the values for which  $\gamma = 1$ , the "so-called"  $\Theta$  point for both lattices. Thus, the fits for  $\Phi = 0.29$  in Table I and for  $\Phi = 0.125-0.130$  in Table II may be in error because the values of  $N$  used may be below the region in which eq 17 and 18 apply. If this is true, the fitted values of  $\gamma_R$  and  $\gamma_S$  would appear to be too large, so the fitted values are upper bounds to the true values.

For these large values of  $\Phi$  (i.e., lower temperatures), not only are eq 17 and 18 not obeyed, but also the proportionality of  $\langle R^2 \rangle$  to  $\langle S^2 \rangle$  is lost. This is illustrated in Figure 8 that shows  $\langle R^2 \rangle / \langle S^2 \rangle$  vs.  $N$  on a logarithmic scale for the simple cubic lattice for  $\Phi = 0$ , 0.25, and 0.5. The curves for  $\Phi = 0$  and 0.25 give constant values for  $\langle R^2 \rangle / \langle S^2 \rangle$ , while the curves for  $\Phi = 0.5$ , which is greater than the  $\Theta$  point, do not approach a constant value. In fact, no simple relationship for either  $\langle R^2 \rangle$  or  $\langle S^2 \rangle$  above the  $\Theta$  point has been found.

The ratio of the constants of proportionality,  $A/B$ , for both lattices is plotted vs.  $\Phi$  in Figure 9. The deviation of  $A/B$  from 6, the value of  $\langle R^2 \rangle / \langle S^2 \rangle$  for the random coil, is small but beyond experimental error.

**Reduced Moments of Distributions in  $R^2$  and  $S^2$ .** The distribution of  $R^2$  has been discussed before<sup>5</sup> for nonintersecting chains with values of  $\Phi$  between 0 and  $\Phi_c$ . This distribution is of special interest since it is used in estimating light-scattering data.<sup>10</sup> In fact, a good deal of the previous Monte Carlo work has been directed in obtaining

an approximate expression for this distribution by estimating moments<sup>5,11</sup> of  $R^2$ . We shall present here the moments obtained from our calculations for both  $R^2$  and  $S^2$ .

The average values of the moments of  $R^2$  and  $S^2$  are defined as

$$\langle R^p \rangle = \langle (R^2)^{p/2} \rangle \quad (19)$$

and

$$\langle S^p \rangle = \langle (S^2)^{p/2} \rangle \quad (20)$$

where the averages of the chains are taken by eq 11. We report here the reduced moments

$$\delta_R(p, s) = \langle R^p \rangle / \langle R^s \rangle^{p/s} \quad (21)$$

and

$$\delta_S(p, s) = \langle S^p \rangle / \langle S^s \rangle^{p/s} \quad (22)$$

In Figures 10-15 we present  $\delta_R(4,2)$ ,  $\delta_S(4,2)$ ,  $\delta_R(6,2)$ ,  $\delta_S(6,2)$ ,  $\delta_R(1,2)$ , and  $\delta_S(1,2)$  vs.  $N$  on a reciprocal scale for  $\Phi = -\infty$ , 0.15 and 0.275 in the simple cubic lattice. These reduced moments are extrapolated to  $N = \infty$ . Despite the uncertainties of the extrapolation, all of the infinite-chain reduced moments are seen to be nearly constant for values of  $\Phi$  from  $-\infty$  to 0.15, but to change appreciably as  $\Phi$  varies from 0.15 to 0.275. The value of  $\delta_R(4,2)$  and  $\delta_S(6,2)$  presented by Flory<sup>12</sup> for random coils as a function of chain length  $N$  are shown by dashed lines in Figures 10 and 12. The reduced moments for the random coil are seen to reach their limiting value with increasing chain length  $N$  much more rapidly than the moments for chains with excluded volume.

Only the infinite chain values of the reduced moments shown in Figures 11, 13, 14, and 15 for the random coil are easily available; these values are indicated by dashed lines in the figures. The infinite-chain random-coil values

(10) D. McIntyre, J. Mazur, and A. M. Wims, *J. Chem. Phys.*, **49**, 2887 (1968).

(11) S. D. Stellman and P. J. Gans, *IUPAC Int. Symp. Macromol., Helsinki, Finland, Prepr.* **3**, 313.

(12) E. Loftus and P. J. Gans, *J. Chem. Phys.*, **49**, 3828 (1968).

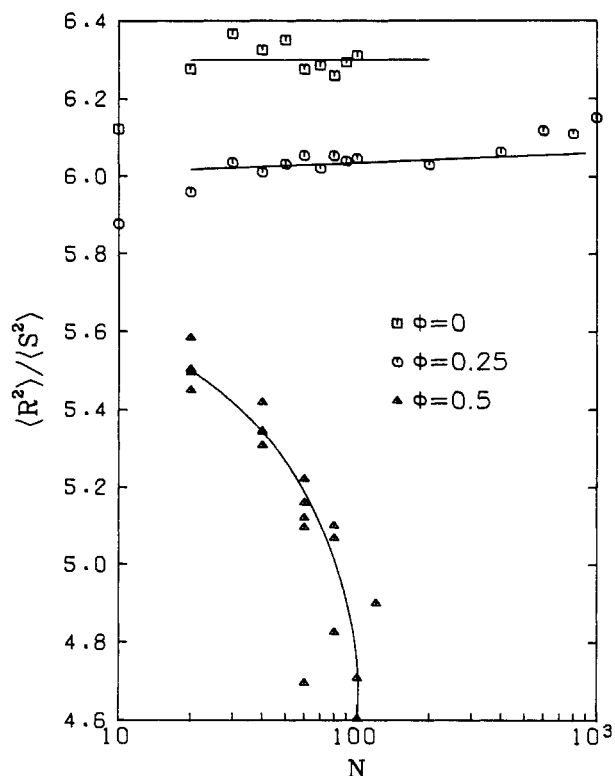


**Figure 8.** The ratio  $\langle R^2 \rangle / \langle S^2 \rangle$  vs.  $N$  for three energies on the simple cubic lattice. Notice that for  $\Phi < \Phi_c$  ( $\Phi_c = 0.267$ ),  $\langle R^2 \rangle / \langle S^2 \rangle$  is independent of  $N$  for large enough  $N$  while for  $\Phi = 0.5$ , the ratio is strongly  $N$  dependent.

of  $\delta_S(4,2)$  and  $\delta_S(6,2)$  were determined by Fixman,<sup>13</sup>  $\delta_R(1,2)$  is given by Flory,<sup>14</sup> and we obtained  $\delta_S(1,2)$  by an independent Monte Carlo calculation.

As  $\Phi$  increases from 0 toward  $\Phi_c$  all the infinite-chain reduced moments for chains with excluded volume approach the corresponding values for the random coil. The value of  $\Phi$  for which the extrapolated reduced moments of both  $R^2$  and  $S^2$  equal the random-coil values seems to be slightly larger than 0.275 for the simple cubic lattice.

**Partition Function.** The partition function for the chain, as defined by eq 9, increases with chain length  $N$ , while the partition function per segment,  $f_{ps}$ , given by the  $N$ th root of the partition function for the chain, is found to rapidly approach a limiting value with increasing chain length. In Figure 16 the limiting partition function per segment is shown vs.  $\sigma\Phi$  for both lattices. The total partition function for a random coil of  $N$  segments is  $(\sigma + 1)\sigma^{N-1}$ , where  $\sigma + 1$  is the coordination number of the lattice. Because we have normalized all our partition functions by dividing them by  $(\sigma + 1)\sigma^{N-1}$  (see eq 8 and 12), the partition function for the random coil, and therefore also the partition function per segment for the random coil, is 1. The limiting partition function per segment is seen to equal the random-coil value for  $\Phi = 0.242$  for the simple cubic lattice and for  $\Phi = 0.106$  for the face-centered cubic lattice.

Other thermodynamic functions of the chains have been computed and will be reported in a later paper. Only the partition function per segment is reported here.

## Discussion

**$\Theta$  Point.** The so-called  $\Theta$  point<sup>8</sup> is viewed by most polymer chemists as the condition of temperature and solvent

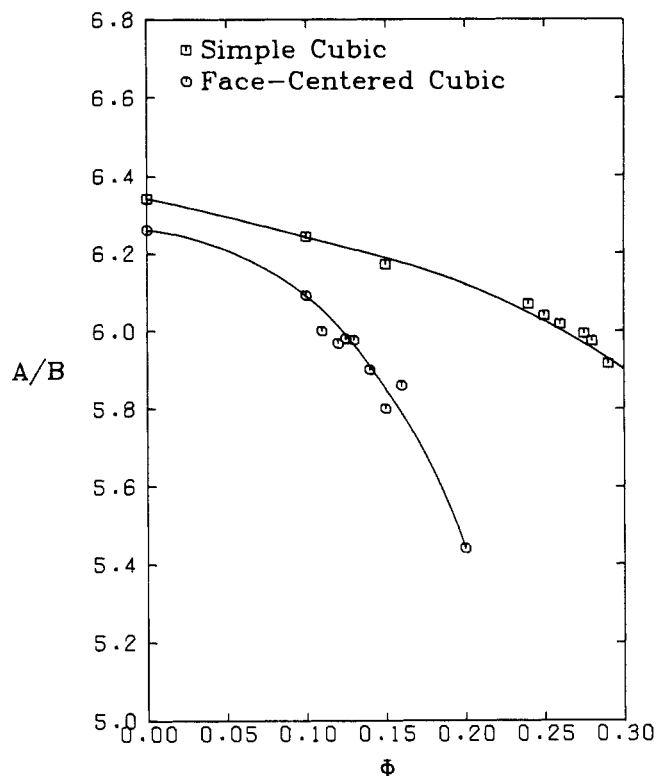


**Figure 9.** The ratio  $A/B$  vs.  $\Phi$  for chains on the simple cubic and face-centered cubic lattices.

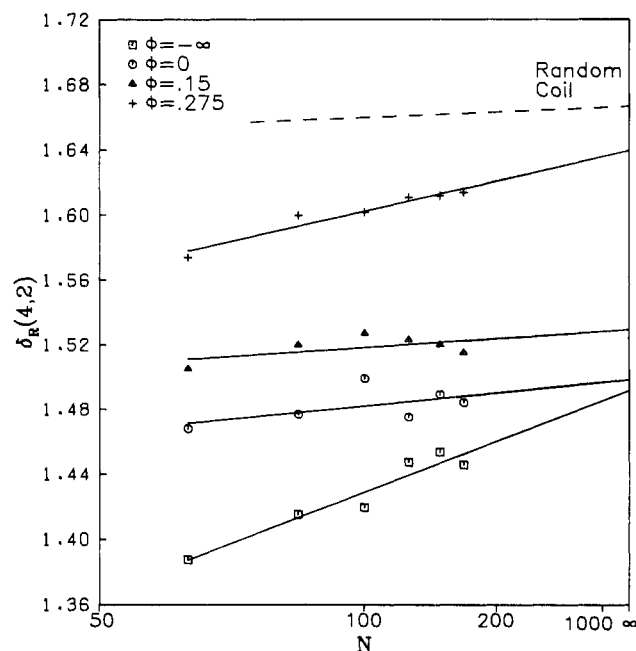


**Figure 10.** The fourth reduced moment of  $R^2$ ,  $\delta_R(4,2)$ , vs.  $N$  on a reciprocal scale for various values of  $\Phi$  for chains on the simple cubic lattices. The dashed line is the value of the reduced moment for the random-coil chain.

at which the attractive energies between segments of a dissolved polymer compensate for the excluded volume effect so that the polymer behaves as if it were a random chain without the excluded volume effect and without attractive energies. In this paper the random chain without the excluded volume effect and without attractive energies is referred to as a random coil. Traditionally, the theta point has two definitions which are not necessarily

(13) S. D. Stellman and P. J. Gans, *Macromolecules*, **5**, 516 (1972).

(14) See ref 5, p 314.

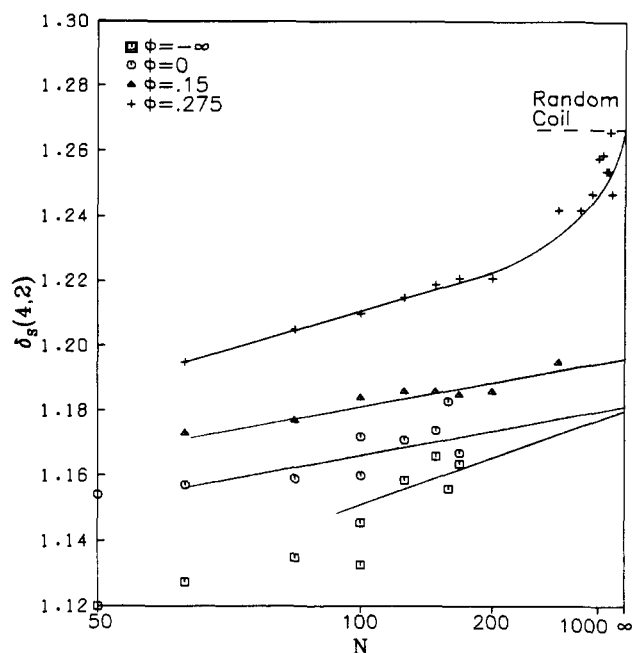


Figure 11. The fourth reduced moment of  $S^2$ ,  $\delta_S(4,2)$ , vs.  $N$  on a reciprocal scale for values of  $\Phi$  for chains on a simple cubic lattice. The dashed line is the value of the reduced moment for the random-coil chain.

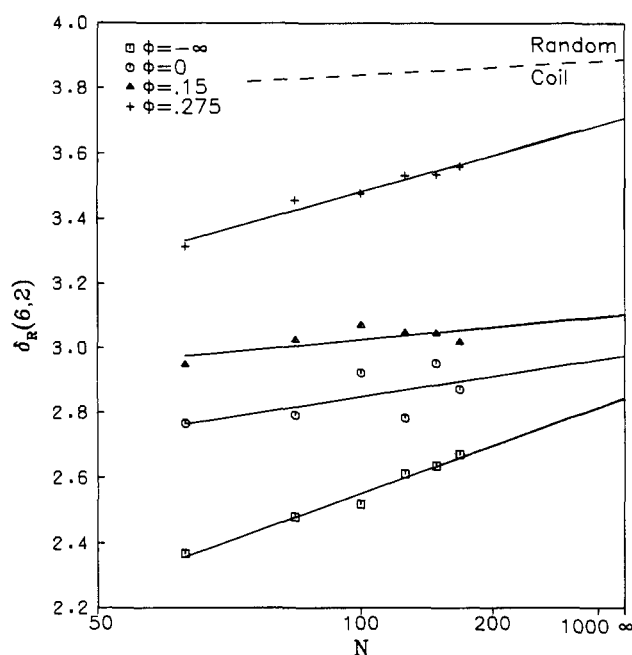


Figure 12. The sixth reduced moment of  $R^2$ ,  $\delta_R(6,2)$ , vs.  $N$  on a reciprocal scale for various values of  $\Phi$  for chains on the simple cubic lattice. The dashed line is the value of the reduced moment for the random-coil chain.

consistent (but which are the same in Flory's theory):<sup>8</sup> (1) the point at which an isolated polymer molecule behaves as a random coil and (2) the point at which the second virial coefficient of the polymer solution vanishes. The first definition deals with a single molecule and will be discussed here with regard to the present Monte Carlo calculations, while the second definition is in terms of solution properties involving interactions between molecules so it cannot be coped with here.

From the present calculations, the mean-square end-to-end distance  $\langle R^2 \rangle$  and the mean-square radius of gyra-

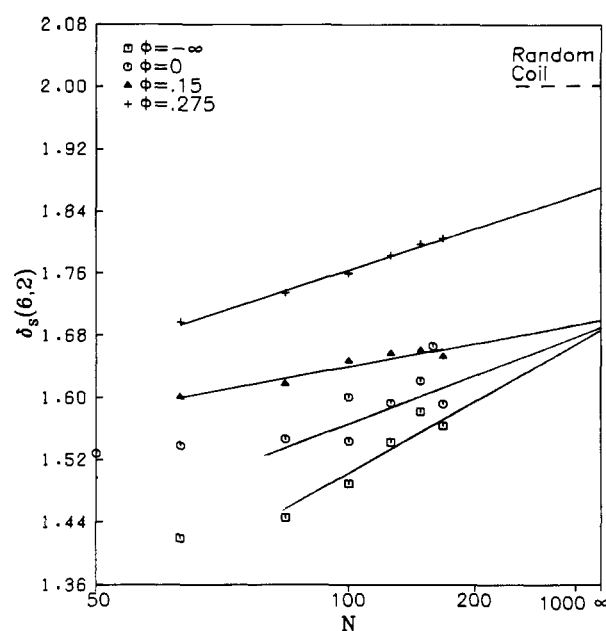


Figure 13. The sixth reduced moment of  $S^2$ ,  $\delta_S(6,2)$ , vs.  $N$  on a reciprocal scale for various values of  $\Phi$  for chains on the simple cubic lattice. The dashed line is the value of the reduced moment for the random-coil chain.

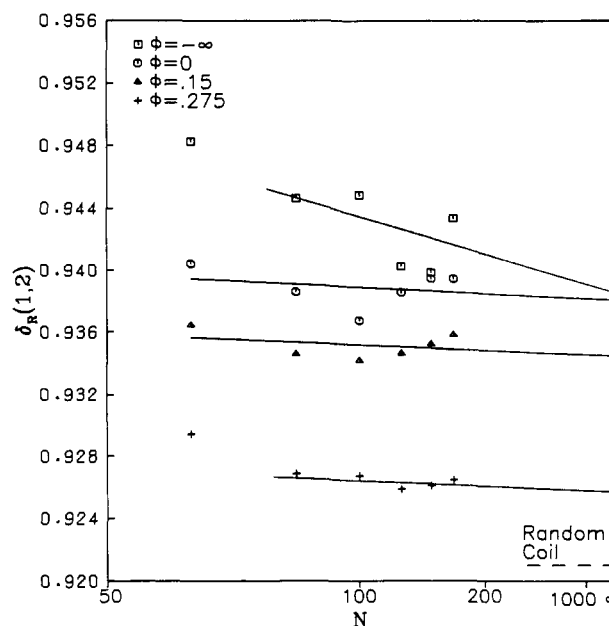


Figure 14. The first reduced moment of  $R^2$ ,  $\delta_R(1,2)$ , vs.  $N$  on a reciprocal scale for various values of  $\Phi$  for chains on the simple cubic lattice. The dashed line is the value of the reduced moment for the random-coil chain.

tion  $\langle S^2 \rangle$  were computed. Moments of  $R^2$  and  $S^2$  and the partition function of the chains were also computed. In what follows these parameters for various values of  $\Phi$  (attractive energy between segments) and their variation with chain length will be compared with the corresponding parameters of a random coil. If they were all equal to those of the random coil for a single critical value of  $\Phi$ , then the existence of a unique  $\Theta$  point,  $\Phi_c$ , by the first definition would be justified. However, as we shall see, slightly different values of  $\Phi_c$  are required for various parameters of our model of self-interacting chains and random coils to agree, so that the theta point can be defined as a range in values of  $\Phi$ .



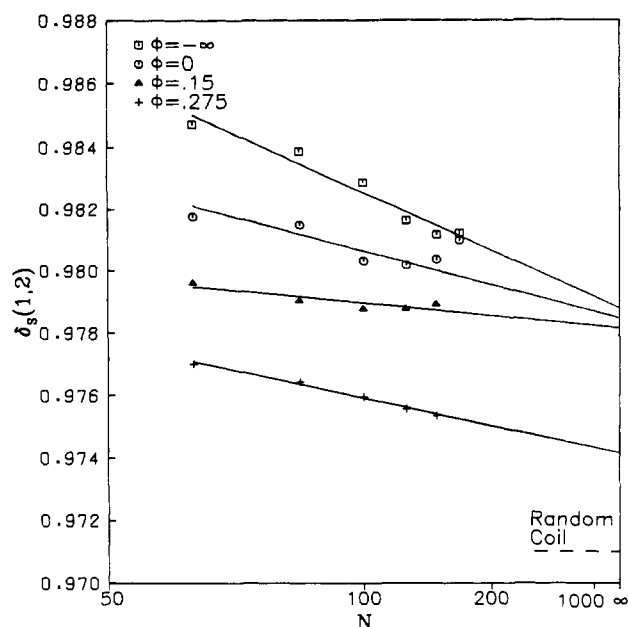


Figure 15. The first reduced moment of  $S^2$ ,  $\delta_S(1,2)$  vs.  $N$  on a reciprocal scale for various values of  $\Phi$  for chains on the simple cubic lattice. The dashed line is the value of the reduced moment for the random-coil chain.

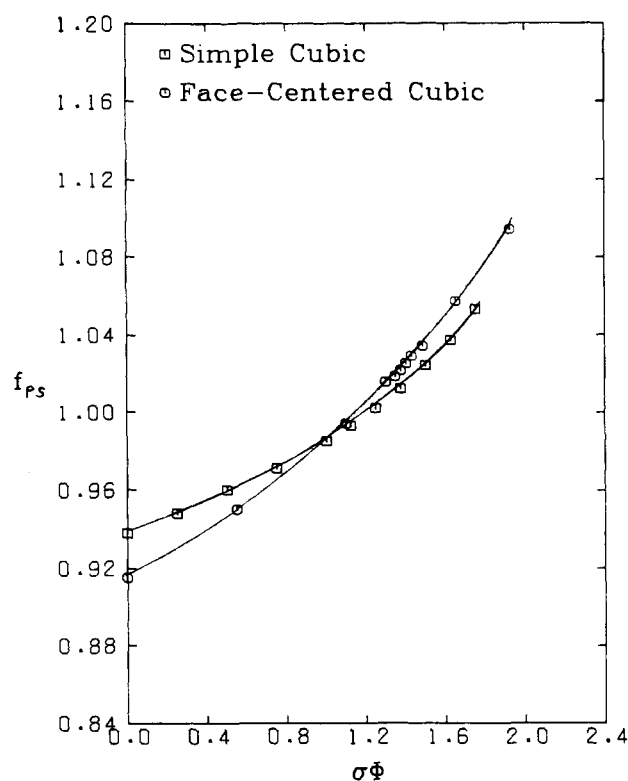


Figure 16. The limit for infinite chains of  $f$  the partition function per segment vs.  $\sigma\Phi$  for the simple cubic and face-centered cubic lattices.

According to eq 5 and 6,  $\langle R^2 \rangle$  and  $\langle S^2 \rangle$  vary as  $N^\gamma$  for the chains with excluded volume, where  $\gamma$  is a function of  $\Phi$ . From Tables I and II,  $\gamma$  is seen to have its random-coil value of one at  $\Phi_c = 0.275$  for the simple cubic lattice and at  $\Phi_c = 0.124$  for the face-centered cubic lattice.

In order that  $\langle R^2 \rangle$  and  $\langle S^2 \rangle$  assume their random-coil values the coefficients  $A$  and  $B$  in eq 5 and 6 must also agree with their values in eq 1-4 for the random coil. By

Table III  
Values of  $\Phi$  for Which Various Parameters of Chains with Excluded Volume and Attractive Energies Have Their Random Coil Values, i.e.,  $\Theta$  Values of  $\Phi$

Parameter	$\Theta$ Value of $\Phi$ for		
	Simple Cubic Lattice	Face-Centered Cubic Lattice	Parameter for Random Coil
Partition function per segment	0.242	0.106	1
$A/B$	0.267	0.117	6
$\gamma$	0.275	0.124	1
Reduced moments	>0.275 See Table IV		

interpolation of Table I, the coefficients  $A$  and  $B$  for the simple cubic lattice  $A$  are both found to assume their random-coil values of 1.5 and 0.25, respectively, at  $\Phi_c = 0.267$ . Likewise, from Table II for the face-centered cubic lattice,  $A$  and  $B$  are both found to assume their random-coil values at  $\Phi_c = 0.117$ .

The values of  $A$  and  $B$  are of course dependent on the lattice. However, their ratio  $A/B = \langle R^2 \rangle / \langle S^2 \rangle = 6$  for random coils in all regular lattices. We conjecture that the ratio  $A/B$  will show a similar independence of the lattice for our chain model. To test this conjecture, in Figure 9,  $A/B$  is plotted vs.  $\Phi$  for both lattices. The ratio is seen to vary only slightly with  $\Phi$  and to have the random-coil value of 6 for  $\Phi = 0.267$  and 0.117 for the simple cubic and face-centered cubic lattices, respectively. Thus ratio  $A/B$  have a different so called theta point than the exponent  $\gamma$ .

Another criterion of the  $\Theta$  point is that the distribution, and therefore the reduced moments, of  $R^2$  and  $S^2$  should be the same at the  $\Theta$  point as for the random coil. For the simple cubic lattice, the reduced moments extrapolated to infinite chain lengths have been seen to have their random-coil values for values of  $\Phi_c$  slightly larger than 0.275.

Another criterion of the  $\Theta$  point is that the partition function per segment in the limit of an infinite chain is equal to 1, the value for the random coil. In the section on Partition Function this was seen to occur at  $\Phi_c = 0.242$  and  $\Phi_c = 0.106$  for the simple cubic and face-centered cubic lattices, respectively, so that the partition function gives a theta point at a lower value of  $\Phi_c$  than for the other properties. These  $\Theta$  values are summarized in Table III.

Thus no unique value of  $\Phi$  exists at which the chains with excluded volume and attractive energies behave as a random coil with respect to the observed dimensional properties. Instead, these quantities assume their random-coil values within a rather narrow range  $\Phi$ . Therefore, a single  $\Theta$  point is not obtained for all properties of the chains.

**Master Curves.** By Tables I and II,  $\gamma$  is seen to equal 1.2 at  $\Phi = 0$  for both lattices, but to decrease with  $\Phi$  more rapidly for the face-centered than for the simple cubic lattice. This is due to the large coordination number of the face-centered cubic lattice that allows each segment to form more contacts.

Our results show that a smaller energy per contact,  $-\epsilon$ , and therefore a smaller value of  $\Phi$  is required for the face-centered cubic lattice to produce the same effect on the dimensions of the chains than for the simple cubic lattice. This suggests plotting  $\gamma$ , which depends on the dimensions of the chains, vs. some function of the coordinate number of the lattice and of  $\Phi$  to obtain a master curve for  $\gamma$  that would apply to chains on all lattices. The cho-

sen function was  $\sigma\Phi$ , where  $\sigma$  is the number of possible choices for a step on the lattice and is one less than the coordination number of the lattice. Thus,  $\sigma = 11$  and  $5$  for the face-centered and simple cubic lattices, respectively. Figure 17 shows values of  $\gamma$  for these two lattices and also for the body-centered cubic lattices for which  $\sigma = 7$ , plotted vs.  $\sigma\Phi$ . The values of  $\gamma$  for all three lattices are seen to lie close to a single master curve. Further calculations on other lattices are required to determine whether the master curve of Figure 17 applies to all lattices and, hopefully, to real polymer molecules.

**Precipitation Phenomenon.** As one increases the attractive energy between segments, one might expect the chain to finally collapse upon itself. This phenomenon might be viewed as a single-chain precipitation. We have studied this phenomenon with special interest to see (1) if the precipitation occurs over a narrow temperature range as a phase phenomenon and (2) if there is a sharp precipitation, how does it relate to the  $\theta$  point.

Figure 18 shows a plot of  $\langle S^2 \rangle / N$ , the radius of gyration squared per chain segment for various chain lengths, as a function of  $\Phi$  for the simple cubic lattice. We have used the radius of gyration since it is a direct measure of the size of the polymer. As one goes from small  $N$  to larger  $N$  there is an increasing steepness in the  $\langle S^2 \rangle / N$  vs.  $\Phi$  plot. For  $N = 1000$  the steepness of the descent is impressive suggesting that for long enough chains there is truly a discontinuity in the radius of gyration corresponding to a precipitation point of the chain.

Inspection of Figure 18 suggests that the precipitation point is very near the theta region. Clearly we need more data as a function of energy around the  $\Phi$  region. In a later paper we shall present more data relating to this point. Suffice it to say here, the data are suggestive but not conclusive proof of single-chain precipitation.

**Correspondence between Chains on a Lattice and Polymers in Solution.** Certain properties of long chains on lattices have been found to be independent of the lattice. We propose that these properties will also apply to chains that are not constrained to a lattice, including real polymers in solution.

Monte Carlo calculations of chains that are not constrained to a lattice have been performed by Loftus and Gans,<sup>15</sup> Stellman and Gans,<sup>16</sup> and Warvari, Kraell, and Scott.<sup>4</sup> These chains are not allowed to intersect themselves but do not have attractive energies between segments, so  $\Phi = 0$  for their chains.

Stellman and Gans conclude that  $\langle R^2 \rangle$  and  $\langle S^2 \rangle$  ( $G^2$  in their notation) satisfy eq 17 and 18 but that  $\gamma_R$  is not equal to  $\gamma_S$ , while for chains on a lattice we found that  $\gamma_R = \gamma_S$  for a value of  $\Phi$  which is smaller than  $\Phi_c$ . We have analyzed their data for  $N = 30$ –298 given in Table I in ref 16 by fitting their data assuming first that  $\gamma_R$  is different than  $\gamma_S$  and then assuming that  $\gamma_R = \gamma_S$ . Fitting  $\langle R^2 \rangle$  to eq 17 gave a coefficient of variation of 3.34% and fitting  $\langle S^2 \rangle$  to eq 18 gave a coefficient of variation of 3.46%. When  $\langle R^2 \rangle$  and  $\langle S^2 \rangle$  were fitted with the condition that  $\gamma_R = \gamma_S = \gamma$ , a coefficient of variation of 3.42% with a  $\gamma$  of 1.23 was obtained. Therefore, we believe that their data are consistent with  $\gamma_R$  being equal to  $\gamma_S$ . We have similarly analyzed some of the data given by Loftus and Gans with similar conclusions.

Stellman and Gans also performed a linear regression of  $\log (\langle S^2 \rangle / \langle R^2 \rangle)$  with  $\log (N)$  (Figure IV of ref 12) and found a significant correlation between these quantities.<sup>16</sup> However, the linear regression assumes equal accuracy of all

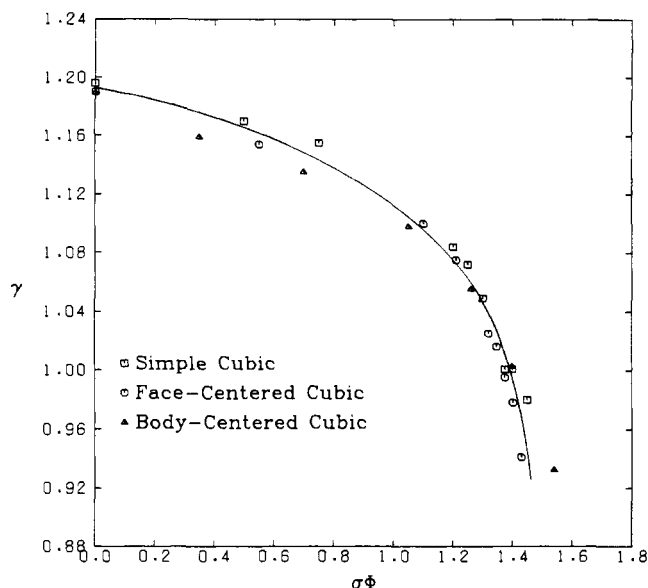


Figure 17. The values of  $\gamma$  vs.  $\sigma\Phi$  for the simple cubic, face-centered cubic, and body-centered cubic lattices.

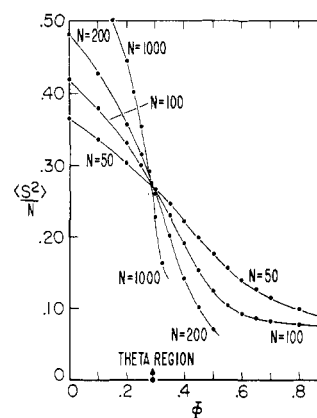


Figure 18. Radius of gyration squared per chain segment vs.  $\Phi$ . The increasing slope of the curves for increasing chain length,  $N$ , indicates precipitation of the chain.

values of  $\log (\langle S^2 \rangle / \langle R^2 \rangle)$ , while these values are much less accurate for their longest calculated chain of  $N = 298$ , as can be seen from their Table I. Because the correlation depends mainly on the value of  $N = 298$ , we do not consider their test to be conclusive.

Warvari, Kraell, and Scott<sup>4</sup> find  $\gamma_R$  equal to  $\gamma_S$  ( $b$  and  $b'$  in their notation) within the statistical reliability of their data.

Grishman<sup>17</sup> recently generated off-lattice chains of up to 500 steps. He found that  $\gamma_R$  was very close to 1.2, in agreement with on-lattice chains for  $\Phi = 0$ , but that a larger value of  $\gamma_R$  was calculated for shorter chains. That is, very long chains are required to determine the limiting value of  $\gamma_R$ . This behavior is similar to that found in Table I and II for on-lattice chains with large  $\Phi$ .

In conclusion, we believe the equality or nonequality of  $\gamma_R$  and  $\gamma_S$  for chains not confined to a lattice has not as yet been determined.

**Distribution of  $R^2$  and  $S^2$ .** In an earlier paper<sup>5</sup> the reduced moments of  $R^2$  were used to fit  $R^2$  to a two-parameter distribution function for values of  $\Phi \leq \Phi_c$ . These results were duplicated by the data of this paper so will not be repeated here.

(15) M. Fixman, *J. Chem. Phys.*, **36**, 306 (1962).

(16) P. J. Flory, "Principles of Polymer Chemistry," Cornell University Press, Ithaca, N. Y., 1953, p 408.

(17) W. W. Mullins in "Metal Surfaces: Structure, Energetics and Kinetics," American Society for Metals, Metals Park, Ohio, 1963.

Similarly we have looked at the reduced moments of  $S^2$  with an eye to obtaining a distribution function for  $S^2$ . Thus far we have been unable to find a distribution function of a simple form over the range of energies for which  $S^2$  was computed. We therefore have abandoned any effort to obtain a distribution function for  $S^2$ , but we use these moments to give some qualitative idea about the distribution. In Table IV we give the estimated values of the reduced moments for infinite chain length for the simple cubic lattice.

The distribution of  $R^2$  and  $S^2$  may be characterized by the reduced second moment around the mean,  $\mu_2$ , which measures the breath of the distribution relative to  $\langle R^2 \rangle$  or  $\langle S^2 \rangle$  and the reduced third moment around the mean,  $\mu_3$ , which measures the skewness.  $\mu_2$  and  $\mu_3$  are given as

$$\mu_{2i} \equiv \delta_i(4,2) - 1 \quad (23)$$

and

$$\mu_{3i} \equiv \delta_i(6,2) - 3\delta_i(4,2) + 2 \quad (24)$$

where  $i = R$  or  $S$ . Values of  $\mu_{3R}$  and  $\mu_{3S}$  are given in Table IV. The values of  $\mu_{2R}$  and  $\mu_{2S}$  may be found by subtracting 1 from corresponding values of  $\delta(4,2)$ . For comparison, the reduced moments for the random coil are also given.

The breadths of both of the distributions,  $\mu_{2R}$  and  $\mu_{2S}$ , are seen to be less than the random-coil values for small attractive energies, and to increase with  $\Phi$  until it reaches the random-coil values at the  $\Theta$  point ( $\Phi = 0.28$ ). However the skewness  $\mu_3$  for the distribution of both  $\langle S^2 \rangle$  and  $\langle R^2 \rangle$  are nearly 0 within the accuracy of the data for all energies below  $\Phi = 0.275$ . The skewness of the distribution of the random coil is of the same order of magnitude. Thus the skewness is small for all energies up to and including the  $\Theta$  region.

## Summary

Properties of polymer chains in solution at the limit of infinite dilution on two lattice models were computed by Monte-Carlo calculations by the R&R method. By weighting the chains by Boltzmann's factors,  $\langle R^2 \rangle$  and  $\langle S^2 \rangle$  were calculated for attractive energies between the chain segments, thus simulating the effects of solvent and temperature.

The computer time required to perform these calculations was reduced by use of an efficient method given in Appendix A of computing the radius of gyration  $\langle S^2 \rangle$  of the chains.

The precision of the parameters calculated for chains generated by the R&R method is best near the  $\Theta$  point. In fact, precise values were obtained near the  $\Theta$  point for chains of 2000 segments. The bias of the parameters calculated by the R&R method was discussed in Appendix B and found to be negligible for the reported parameters.

A wide range of attractive energies was used. Chains for infinite repulsive energies, *i.e.*, chains that were not allowed to form contacts, were generated. Chains on the simple cubic lattice with infinite attractive energy are considered in Appendix D. The chains are shown to be in the shape of cubes so that their radii of gyration could be calculated. Thus, the complete range of interaction energies between segments from infinite repulsive to infinite attractive energies was covered.

The values of  $\langle R^2 \rangle$  and  $\langle S^2 \rangle$  were found to be very inaccurate for chains with large attractive energies, *i.e.*, large values of  $\Phi$ . In order to obtain accurate results, two methods of importance sampling were developed by which accurate results were obtained for values of  $\Phi$  up to 1 at chain lengths up to 100 segments. From the variation of

Table IV  
Extrapolated Values of Reduced Moments for  $R^2$  and  $S^2$   
(Eq 21 and 22) for the Simple Cubic Lattice<sup>a</sup>

	$\Phi = -\infty$	$\Phi = 0$	$\Phi = 0.15$	$\Phi = 0.275$	Random Coil
$\delta_R(1,2)$	0.94	0.94	0.94	0.93	0.921
$\delta_S(1,2)$	0.97	0.98	0.98	0.98	0.971
$\delta_R(4,2)$	1.50	1.50	1.52	1.64	1.666
$\delta_S(4,2)$	1.18	1.19	1.20	1.26	1.266
$\delta_R(6,2)$	2.9	3.0	3.1	3.7	3.88
$\mu_{3R}$	$0.4 \pm 0.3$	$0.5 \pm 0.3$	$0.5 \pm 0.3$	$0.8 \pm 0.4$	0.88
$\delta_S(6,2)$	1.69	1.69	1.70	1.87	2.0008
$\mu_{3S}$	$0.2 \pm 0.3$	$0.1 \pm 0.3$	$0.1 \pm 0.3$	$0.1 \pm 0.3$	0.19

<sup>a</sup> Values of the third reduced moment around the mean for  $\langle R^2 \rangle$ ,  $\langle \mu_{3R} \rangle$ , and  $\langle S^2 \rangle$ ,  $\langle \mu_{3S} \rangle$ , (eq 23 and 24) are also given. Values of the second reduced moment around the mean may be obtained by subtracting one from  $\delta_R(4,2)$  or  $\delta_S(4,2)$ , respectively.

the radius of gyration with  $\Phi$ , evidence for precipitation of a chain at a value of  $\Phi$  near the  $\Theta$  region was found.

The values of  $\langle R^2 \rangle$  and  $\langle S^2 \rangle$  for large  $N$  were found to fit eq 5–7. We interpreted these values of  $\langle R^2 \rangle$  and  $\langle S^2 \rangle$  to obtain a better understanding of the nature of the  $\Theta$  point, the condition of solvent and temperature corresponding to a value of  $\Phi$  for which the chain behaves as a random coil. The values of  $\Phi$  at the  $\Theta$  points for various parameters of the chains are given in Table IV. The  $\Theta$  point is seen to be different for different parameters, so that we concluded unique value of  $\Phi$  for the  $\Theta$  point does not exist.

A master curve for  $\gamma$  was constructed. By plotting  $\gamma$  vs.  $\sigma\Phi$ , where  $\sigma + 1$  is the coordination number of the lattice, a single curve representing three lattices was obtained. This master curve thus appears to be independent of the lattice and hopefully will also apply to real polymers in solution.

## Appendix A

**Calculation of Radius of Gyration.** A method for efficient calculation of the radius of gyration was developed. The squared radius of gyration for a walk of  $N$  steps is

$$S_N^2 = \frac{1}{N+1} \sum_{k=0}^N [(x_k - \bar{x})^2 + (y_k - \bar{y})^2 + (z_k - \bar{z})^2] \quad (A1)$$

where  $x_k$ ,  $y_k$ , and  $z_k$  are the coordinates after the  $k$ th step of the walk and  $\bar{x}$ ,  $\bar{y}$ , and  $\bar{z}$  are the averages of the coordinates over the walk, given by

$$(N+1)\bar{x} = \sum_{k=0}^N x_k$$

$$(N+1)\bar{y} = \sum_{k=0}^N y_k \quad (A2)$$

and

$$(N+1)\bar{z} = \sum_{k=0}^N z_k$$

Equation A1 may be written as

$$(N+1)S_N^2 = \sum_{k=0}^N R_{0,k}^2 - (N+1)(\bar{x}^2 + \bar{y}^2 + \bar{z}^2) \quad (A3)$$

where

$$R_{0,k}^2 = x_k^2 + y_k^2 + z_k^2 \quad (A4)$$

is the square of the distance from the beginning of the walk to the end of the  $k$ th step.

Calculation of  $R_{0,k}^2$  by eq A4 for each step of the chain required considerable time on the computer. Therefore, a more efficient method of calculating  $R_{0,k}^2$  was developed as follows.

By changing subscripts and expanding, eq A4 gives

$$R_{0,j+1}^2 - R_{0,j}^2 = 2(x_j\Delta x_j + y_j\Delta y_j + z_j\Delta z_j) + (\Delta x_j)^2 + (\Delta y_j)^2 + (\Delta z_j)^2 \quad (\text{A5})$$

where

$$\Delta x_j = x_{j+1} - x_j, \text{ etc.} \quad (\text{A6})$$

For a step on a simple cubic lattice, two of the quantities  $\Delta x_j$ ,  $\Delta y_j$ , and  $\Delta z_j$  are 0 and the other one is +1 or -1, so that eq A5 becomes

$$R_{0,j+1}^2 - R_{0,j}^2 = 2(x_j\Delta x_j + y_j\Delta y_j + \Delta z_j\Delta z_j) + 1 \quad (\text{A7})$$

Summing from  $j = 0$  to  $j = k - 1$  gives

$$R_{0,k}^2 = 2 \sum_{j=0}^{k-1} (x_j\Delta x_j + y_j\Delta y_j + z_j\Delta z_j) + k \quad (\text{A8})$$

The summation is easily performed during generation of the walk, especially since only one term in the summation is non-zero for each step. The summations in eq A2 are also performed during generation of the walk. Then  $S_N^2$  is computed by eq A2, A3, and A8 after the walk is completed. The method was easily modified to apply to the face-centered cubic lattice.

## Appendix B<sup>18</sup>

**Estimation of Bias.** Let  $T$  be the number of possible configurations of chains of a given length. Then the partition function,  $f$ , of the chains is defined as

$$f = \sum_{i=1}^T \exp(P_i\Phi) \quad (\text{B1})$$

where  $P_i$  is the number of contacts (two unbonded segments separated by one lattice distance) in the  $i$ th configuration,  $\Phi = -\epsilon/k_B t$ ,  $\epsilon$  is the energy of a contact,  $k_B$  is the Boltzmann constant, and  $t$  is the temperature. The mean value of a property  $v$  of the chains is defined as

$$\langle v \rangle = \left[ \sum_{i=1}^T v_i \exp(P_i\Phi) \right] / f \quad (\text{B2})$$

Because eq B1 and B2 involve summations over all possible configurations of the chains, their use to calculate  $f$  and  $\langle v \rangle$  is not practical. Therefore  $f$  and  $\langle v \rangle$  are estimated from a sample of configuration of the chains. In this appendix, values estimated by eq 9 and 11 are called  $\hat{f}$  and  $\langle \hat{v} \rangle$  to distinguish them from the true unknown values given by eq B1 and B2.

In ref 9, the estimated partition function  $\hat{f}$  is shown to be unbiased and the bias of the estimate of a property of the chains, the expected value of the estimate minus the true value, is given as

$$B_m = E[\langle \hat{v} \rangle] - \langle v \rangle = -\frac{1}{mf^2} \sum_{i=1}^T (v_i - \langle v \rangle) w_i \exp(P_i\Phi) \quad (\text{B3})$$

The bias  $B_m$  varies inversely with  $m$ , the number of configurations used to estimate  $\langle \hat{v} \rangle$ . In eq B3 the weighting factors  $w_i$  are given by eq 8 rather than eq 12.

Because the summation in eq B3 is over all possible configurations of the chain, it cannot be directly calculated. In this appendix, a practical method of estimating the bias  $B_m$  from the calculations of this paper is given.

To illustrate this method, Monte Carlo data that are expected to have a large bias,  $B_m$ , were obtained. Twenty Monte Carlo runs were made of chains on the simple

cubic lattice with  $\Phi = 0.5$ . In each run, 500 chains of 100 segments each were generated and the mean values of the squared radius of gyration  $\langle \hat{S}^2 \rangle$  vs. the partition function  $\hat{f}$  for each run are shown by the squares on Figure 19. For this large value of  $\Phi$ , the values of  $S^2$  for individual chains deviate greatly from the mean value of  $S^2$  so, by eq B1, the bias term is expected to be large. Despite the large scatter of the data, these quantities are seen to be correlated; large values of  $\hat{f}$  correspond to small values of  $\langle \hat{S}^2 \rangle$ . This relationship for any parameter  $v$  is measured by the covariance given as

$$\text{covar}(\langle \hat{v} \rangle \hat{f}) = \frac{1}{p-1} \left[ \sum_{i=1}^p \langle \hat{v} \rangle_i \hat{f}_i - \frac{1}{p} (\Sigma \langle \hat{v} \rangle_i)(\Sigma \hat{f}_i) \right] \quad (\text{B4})$$

for  $p$  runs. The covariance of  $\langle \hat{S}^2 \rangle$  and  $\hat{f}$  for the data for Figure 19 is  $-1.18 \times 10^5$ . We now relate the covariance to the bias  $B_m$ .

The covariance of  $\langle \hat{v} \rangle$  and  $f$  may also be expressed in terms of the bias  $B_m$ . By definition

$$\text{covar}(\langle \hat{v} \rangle \hat{f}) = E(\langle \hat{v} \rangle \hat{f}) - E(\langle \hat{v} \rangle)E(\hat{f}) \quad (\text{B5})$$

now

$$\langle \hat{v} \rangle \hat{f} = \frac{1}{m} \sum_{k=1}^m v_k w_k \quad (\text{B6})$$

so that

$$E(\langle \hat{v} \rangle \hat{f}) = E(v_k w_k) = f \langle v \rangle \quad (\text{B7})$$

by eq 9 and 12 of ref 9. Also, by ref 9,

$$E(\hat{f}) = f \quad (\text{B8})$$

Substituting eq B3, B7, and B8 in eq B5 gives

$$B_m = \text{covar}(\langle \hat{v} \rangle \hat{f}) / f \quad (\text{B9})$$

Using the mean value of  $\hat{f}$  for  $f$ , the bias is calculated by eq B4 and B9 to be  $-0.71$  for samples of 500 configurations from the data of Figure 19. This bias is seen to be small compared to the scatter of the data even for these conditions that give a large bias.

Similar data were also obtained using importance sampling. Twenty Monte Carlo runs of 500 chains of 100 segments each were made on the simple cubic lattice for  $\Phi = 0.5$  in which steps in the direction toward the origin were taken with twice the probability of steps away from the origin, i.e., method A (importance sampling) of the text. The averages for the 20 individual runs are plotted as circles in Figure 19. With importance sampling, the values of  $\langle \hat{S}^2 \rangle$  and  $\langle \hat{f} \rangle$  seem to have little if any correlation. Thus the covariance and the bias by eq B4 and B9 are small. Importance sampling has been shown in the text to increase the precision of the estimate of the parameters. In this case, importance sampling is seen to also reduce their bias.

## Appendix C

**Dependence of Precision of Estimates on  $\Phi$ .** The coefficient of variation of  $\langle R^2 \rangle$  is seen by Figure 1 to have a minimum for the simple cubic lattice for  $\Phi$  about 0.25, which is about the value of  $\Phi$  for which the partition function per segment has the value of one. The standard deviation of other calculated parameters of the walks using the R&R method have been found to have a minimum at about the same value of  $\Phi$ . In this appendix we give a heuristic explanation of this minimum.

The estimate of the average value of any parameter  $v_i$  is given by eq 11. For long chains, the factor  $w_k \exp(P_k\Phi)$  may vary by many orders of magnitude among chains while the value of the parameter,  $v_k$ , varies considerably

(18) In this Appendix we have used  $T$  to be the number of configurations and  $t$  to be the temperature to be consistent with the notation in ref 9. Otherwise the notation is consistent with the rest of the paper.

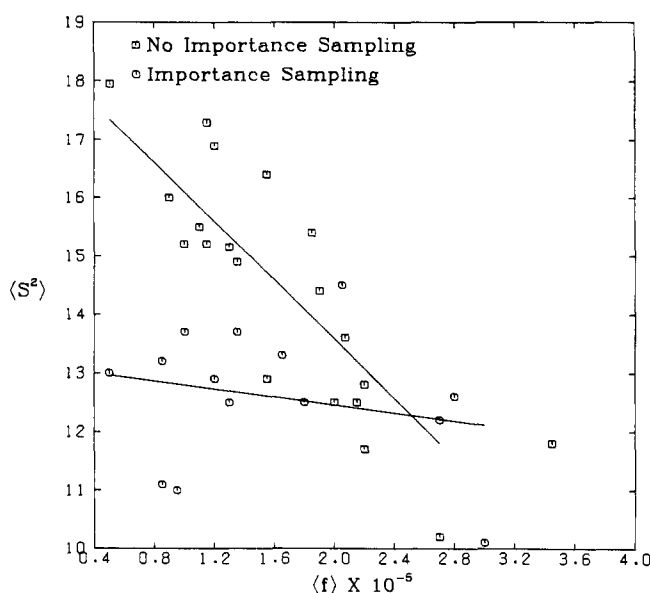


**Figure 19.**  $\langle S^2 \rangle$  vs. the partition function per segment  $\langle f \rangle$  for 20 runs of 500 configurations each on the simple cubic lattice with  $\Phi = 0.5$ . The lines have been fitted by the least-squares method.

less among chains. Then, both the numerator and denominator of eq 11 depend on only those chains with large values of  $w_k \exp(P_k \Phi)$ . Thus, only a small fraction of calculated chains contribute substantially to the average  $\langle v \rangle$ , in some cases only 1/1000, and an inaccurate average is therefore obtained. By this reasoning, the standard deviation of the estimates given by eq 11 should be small when the distribution of total weights  $w_k \exp(P_k \Phi)$  is narrowest. We now determine the value of  $\Phi$  for which this is true.

For a chain generated using R&R method the total weight for the chain by eq 10 and 12 is

$$w_k \exp(P_k \Phi) = \prod_{i=2}^N \left[ \frac{\sigma - C_{ik}}{\sigma} \exp(C_{ik} \Phi) \right] \quad (C1)$$

Now the above equation may be rewritten in terms of the numbers of contacts at each site; for the simple cubic lattice ( $\sigma = 5$ ) we have

$$\prod_{i=2}^N \left[ \frac{5 - C_{ik}}{5} \exp(C_{ik} \Phi) \right] = [1]^{n_{0k}} [(4/5)e^{\Phi}]^{n_{1k}} [(3/5)e^{2\Phi}]^{n_{2k}} [(2/5)e^{3\Phi}]^{n_{3k}} [(1/5)e^{4\Phi}]^{n_{4k}} \quad (C2)$$

where  $n_{jk}$  is the number of sites in the  $k$ th chain with  $j$  nearest-neighbor contacts. Thus

$$\sum_{j=0}^4 n_{jk} = N \quad (C3)$$

There are two simple cases in which  $w_k \exp(P_k \Phi)$  would be nearly constant from chain to chain: (1) the distribution of  $n_{jk}$  does not vary from chain to chain; (2) the terms  $[(5 - j)/5] \exp(j\Phi)$  are nearly equal. It is the latter case that holds for about  $\Phi = 0.25$  as is illustrated in Table V. Most sites have 0, 1, or 2 contacts. For  $\Phi = 0.25$ , the terms  $[(5 - j)/5] \exp(j\Phi)$  are nearly equal to 1 for  $j = 0$ ,

**Table V**  
Product of Weighting Factor and Boltzmann Factor,  $[(5 - j)/5] \exp(j\Phi)$ , for a Site of a Chain in a Simple Cubic Lattice with  $j$  Contacts

	$\Phi$				
$j$	0	0.2	0.25	0.3	0.5
0	1.0	1.00	1.00	1.00	1.00
1	0.8	0.98	1.03	1.08	1.32
2	0.6	0.90	0.99	1.09	1.63
3	0.4	0.73	0.85	0.98	1.79
4	0.2	0.45	0.54	0.66	1.48

1, and 2 so the total weighting factor of all the chains will be near 1. Therefore, all chains will contribute to averages of the parameters and precise averages will be obtained. Similar results were obtained for the face-centered cubic lattice for a  $\Phi$  of about 0.12, using the R&R method to generate chains. For these values of  $\Phi$ , the partition function, eq 8, will be near unity for nearly all the chains.

## Appendix D

**Radius of Gyration of Chains with Infinite Attractive Energy.** For infinite attractive energy between segments, a chain will assume a configuration with the largest possible number of contacts between segments. On a simple-cubic lattice every segment, except the end segment, can participate in a maximum of four contacts. A chain with infinite attractive energies will assume a compact configuration with no voids in the configuration so that every segment not on the surface of the configuration will participate in the maximum of four contacts. On the other hand, segments on the surface will participate in less than four contacts. We will refer to these as missing contacts. The compact chain will thus assume the shape that minimizes the missing contacts of the surface segments.

Determining the shape of a chain of fixed length on a simple-cubic lattice is equivalent to determining the shape of a crystal of a fixed volume on a cubic lattice. A shape of the crystal that minimizes the surface tension (missing surface atomic bonds) will be the shape of the polymer chain that minimizes missing contacts. The shape of the crystal, and therefore also of the chain, has been shown<sup>19</sup> to be a cube with its edges along the coordinates axes. The radius of gyration for a chain in the shape of a cube was evaluated as

$$\langle S^2 \rangle = [(N + 1)^{2/3} - 1]/4 \quad (D1)$$

where  $N$  is the number of segments in the chain so that  $N + 1$  is the number of beads connected by the segments. Formula D1 only applies when the chain can form a complete cube, i.e.,  $N + 1$  is the cube of an integer. The curve for  $\Phi = \infty$  on Figure 3 was calculated by formula D1 for  $N + 1 = 3^3, 4^3, 5^3$ , etc. For values of  $N + 1$  that are not a cube of an integer, the chain cannot form a complete cube so that the value of  $\langle S^2 \rangle$  and  $\Phi = \infty$  will be only approximately given by eq D1.

(19) R. Grishman, *J. Chem. Phys.*, **58**, 220 (1973).